Flexible Radar Channel Model for Multi-Dimensional Radar

T G Pelham, MIEEE, MIET
University of Bristol
UNITED KINGDOM

t.g.pelham@bristol.ac.uk

ABSTRACT

The development of the networked battlespace as a concept, and the wealth of wired and wireless communications to support it have opened the door to truly multidimensional radar systems. Whether as a static network of radars coordinating to provide national coverage, or a local network for UAV's providing a swarm aperture for rapidly reconfigurable airborne radar, there is an urgent need for a flexible radar channel model to empower the engineer and scientist to develop new systems, sensing algorithms and concepts of operation. LyceanEM, an open source electromagnetics model is presented as a solution to this issue, allowing for multi source, heterogeneous antenna arrays to be simulated together with a radar target, and the effects of timing jitter to be explored within the demonstrator system.

1.0 INTRODUCTION

The development of the networked battlespace, and the availability of software defined radios and phased antenna arrays has opened the door to novel radar paradigms [1]. There has been considerable interest on this topic, exploring the dimensions offered by both traditional terrestrial radar in terms of frequency, waveforms, doppler analysis and polarisation [2], and by smaller mobile, multi-static radar systems [3]. These systems are enabled by improved access to embedded computing and software defined radio architectures that are lighter with reduced power consumption. However, capability comes at a cost, and in order to explore the full capabilities of proposed swarm both the proposed algorithm and hardware must be evaluated, while considering the effects of antenna polarisation, beamforming algorithms, propagation and radar cross section in a realistic but accessible way. When considering the effectiveness of different antenna arrays for radar systems, the maximum directivity of a planar array at boresight is well established [4]. However, as new radar systems paradigms are introduced such as multi-static radar systems for detection and tracking [5], [6], or imaging radar [7], [8], [9], the assumption of coherent beamforming using the full array cannot be relied upon. In addition to these proposals, the introduction of MIMO (multiple input, multiple output) radar, and staring radar [10], [11], [12], [13] depends upon an antenna array and transceiver with multiple independent transmit and receive channels. While many of the elements required for this kind of sophisticated radar model can be simulated independently, such as antenna array patterns or radar cross section using CST or HFSS [14], [15], this introduces additional complexity and design effort which would otherwise be dedicated to the main issues of multi-dimensional radar. While there is an excellent open source package for the investigation of tracking algorithms using different sensors in the form of Stone Soup, it does not extend to the inclusion of radio propagation, radar cross section, or antenna array implementation on a platform of interest [16], [17].

In this paper, a flexible radar channel model is introduced that supports the simulation of complex planar and conformal antenna arrays on platform, and both time and frequency domain channel models. LyceanEM is an open source electromagnetics package written in python, and GPU accelerated using Nvidia's CUDA framework to model sensors and communications [18], [19]. This model is built upon a ray tracing architecture, allowing for complex models to be simulated rapidly on a desktop machine. The frequency domain model allows for the consideration of different beamforming architectures, propagation, and radar cross section or intelligent surfaces to be considered quickly in the frequency domain. The time domain model allows for different transmit waveforms to be modelled, together with true time delay beamforming, or time domain MIMO processing, together with all the features offered by the frequency domain model.

In order to illustrate the opportunities which this open source package provides, a small swarm of low cost unmanned aerial vehicles (UAV) will be simulated as a demonstration, with X band conformal antenna arrays mounted on the ventral nose of the UAV. The utility of both frequency and time domain models will be introduced for the detection and analysis of a target UAV of the same design at a range of 2km.

2.0 MODELLING

2.1 Cooperative Radar Scenario

In order to model a multi-dimensional radar problem of interest, a cooperative network of three UAVs was chosen, with the example packaged within LyceanEM selected as the host platform [20]. These UAVs are shown in Figure 1, with the lead UAV designated as the origin, and the followers arranged with a spacing of 500m, offset at 45 degrees either side of their common heading which is designated as the positive x direction with a flight altitude of 2km. For simplicity all UAS are arranged in the same plane. The rendering of the simulation environment for LyceanEM is provided by Open3D. The example UAV design has a total wingspan of 80cm, and an overall length of 50cm. This is meant to represent a small low cost UAV, suitable for short duration missions with a minimal payload.

Figure 1 : Cooperative UAV Swarm, arranged with a spacing of 10m, 45 degrees offset from the shared heading.

The target of interest in this scenario is another identical UAV, situated 2km away from lead UAV, on a bearing of -30 degrees in azimuth, and 0 degrees in elevation, with a heading of 120 degrees in azimuth. This arrangement places the target at a relative range of 2000m from the lead UAV (designated Swarm 1), 2486m from the second UAV (designated Swarm 2), and 2183m from the third UAV (designated Swarm 3). The relative bearings of the target from the UAS are -32.9 degrees in azimuth for Swarm 2, and -17.2 degrees for Swarm 3.

In order to calculate the radar cross section of an arbitrary target in a consistent way, LyceanEM employs discrete raytracing in which all the scattering points to be consider are included in the model. In order to ensure consistent spacing between points on an arbitrary model, Poisson disk sampling is used to arrange the scattering points on the model surface, and this distribution is shown in Figure 2.

In this example each UAV in the swarm is equipped with a conformal X band antenna array comprised of 67 point sources, defined using LyceanEM as vertically polarised antenna elements, conformal with the surface of the antenna array.

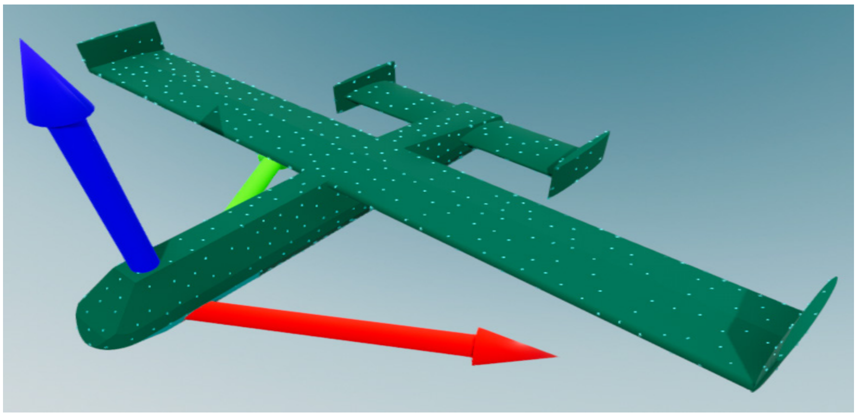

Figure 2: Target UAV, with local origin and discrete scattering points shown as aqua dots.

2.2 Frequency Domain Modelling

The frequency domain channel model was used to simulate a transmission from Swarm 1, allowing for both propagation from the transmitting array to the receivers directly, and via the target of interest. This produces a scattering matrix which can then be used to calculate the effects of different beamforming algorithms. Notable a conventional single channel antenna array with can beamform in the time domain, sweeping out a path of command vectors of interest, with the speed determined by the desired dwell time in any particular direction. A staring radar using a fully digitally populated or MIMO antenna array in order to sample the received signal at each element independently, allowing for all the desired look angles to be considered simultaneously, resolution only limited by the available compute capability.

2.3 Time Domain Modelling

The time domain model requires more parameters to be determined, and for this example a linear frequency chirp was chosen with a bandwidth of 3GHz, sweeping from 8.5GHz to 11.5GHz over a pulse time of 20ns. The pulse power was chosen as 1dBW, suitable for the small UAV used in the example. A sampling frequency of 60GHz was selected for high resolution output. In the same way as the frequency domain model, a time domain scattering matrix was then produced, allowing for different true time delay beamforming algorithms of both the transmitted pulse and the received signals.

3.0 RESULTS

3.1 Frequency Domain Modelling

In the frequency domain, the coherent wavefront steering algorithm was chosen to perform angle of arrival estimation in both elevation and azimuth, as shown in Figure 3 and Figure 4 using the produced scattering matrix of order M,N for M transmitting antennas, N receiving antennas. In this example the transmit and receive command angles were the same for simplicity, but the effects of mismatch between the transmit and receiver vectors could be considered in further work. When the angle of arrival estimation is considered, it is clear that each one of the radars is able to resolve the transmit pulse from Swarm 1, and the return produced by the target, with a clear peak around -60 degrees in azimuth, and -10 degrees in elevation. The horizontal arrangement of the conformal antenna array provides much higher resolution in the azimuth plane, which is clear from Figure 3. In addition, the greater spread in elevation shown in Figure 4 reflects lower dimension of the array in elevation reducing the resolution in this axis, the configuration of each antenna array biased towards azimuth discrimination.

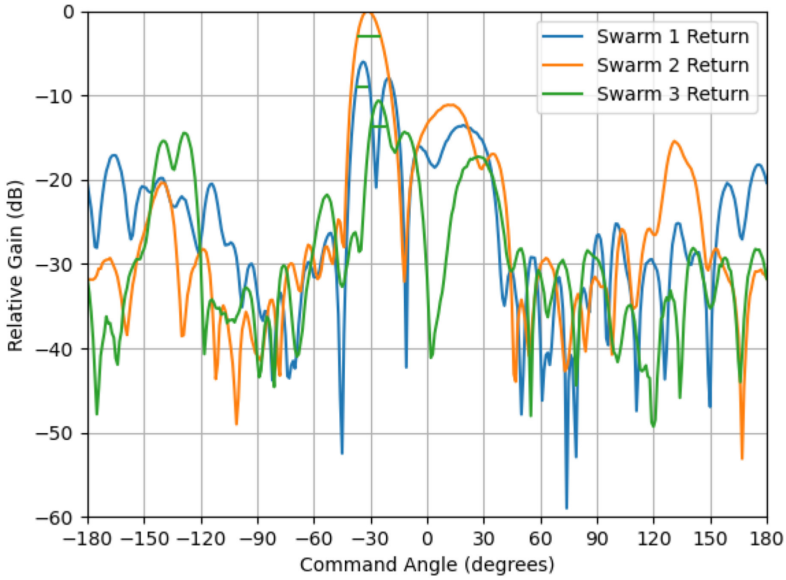

Figure 3: Frequency domain angle of arrival (Azimuth).

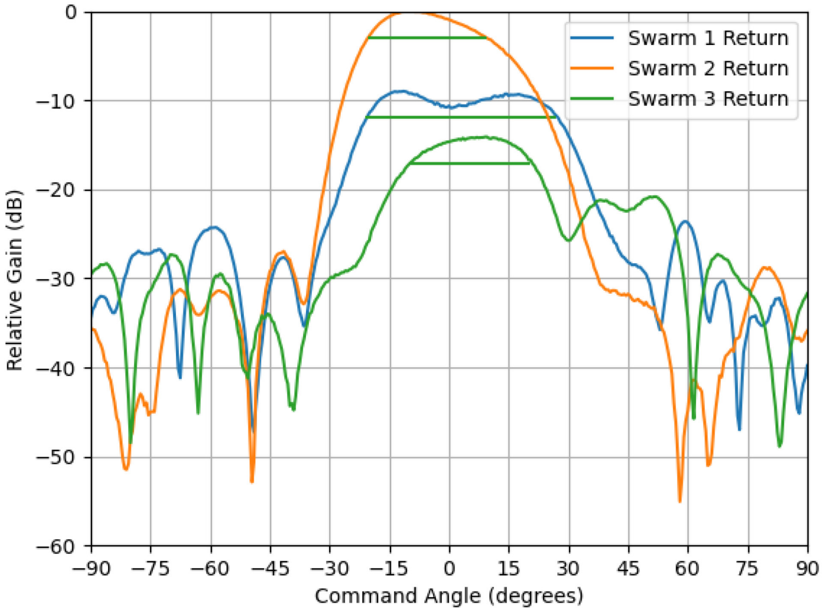

Figure 4: Frequency domain angle of arrival (Elevation).

3.2 Time Domain Modelling

In the time domain, the time domain scattering matrix allows for true time delay beamforming of both the transmitted signal, and for each of the receiving antenna arrays by producing a matrix of order M,N,S for M transmitting antennas, N receiving antennas, and S time domain samples. Once beamforming has been performed the return for each radar can then be considered. The time domain returns were processed using a fast Fourier transform into range bins for each command angle, using time domain beamforming. This example has been sampled for range bins with a length of 50cm, showing the bistatic range bins for each UAS in Figure 5, Figure 6, & Figure 7.

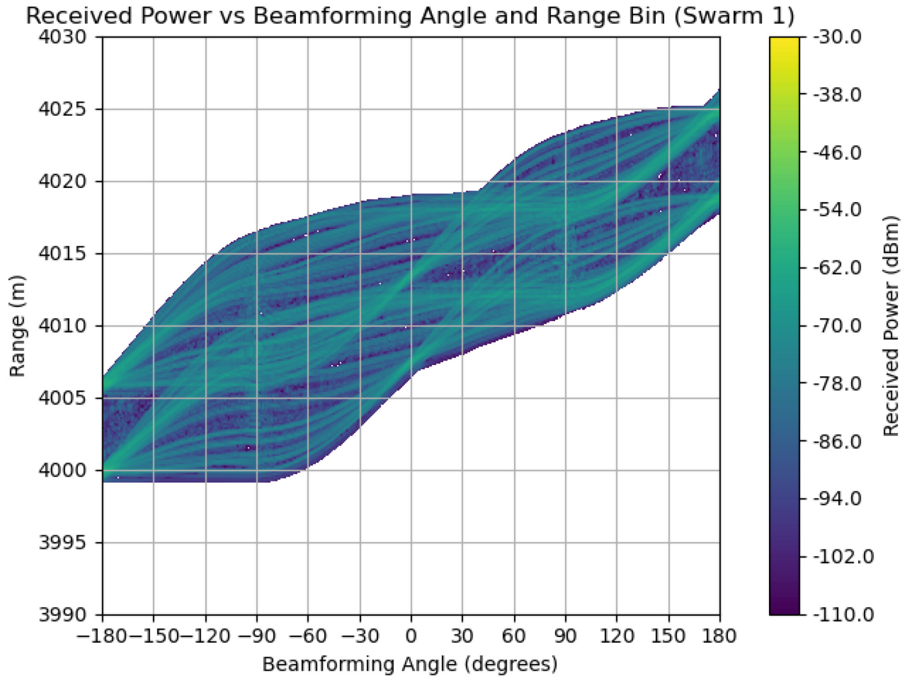

Figure 5: Range vs Azimuth angle for Swarm 1: Received Power.

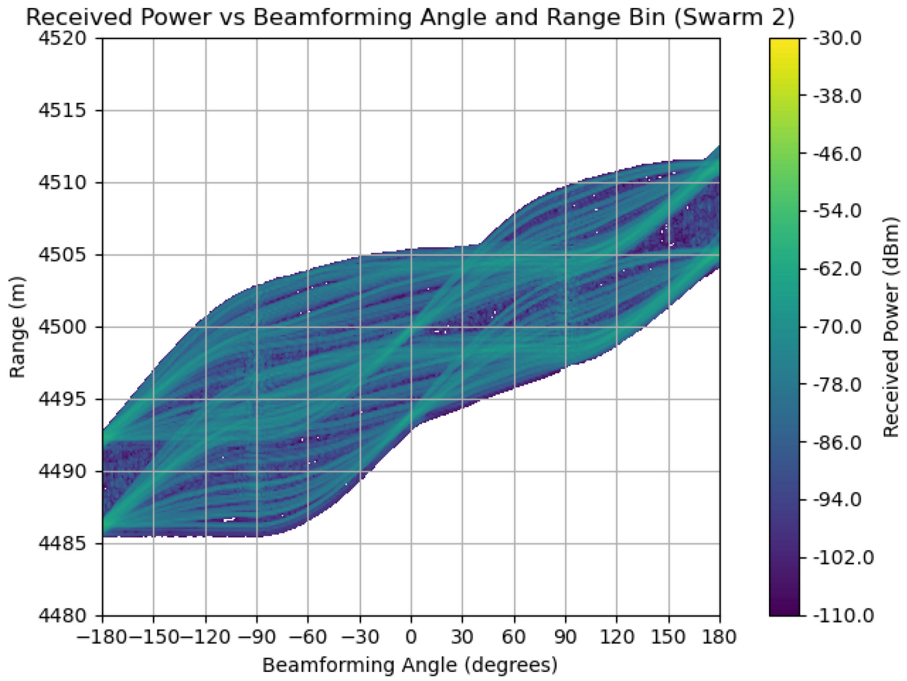

Figure 6: Range vs Azimuth angle for Swarm 2: Received Power.

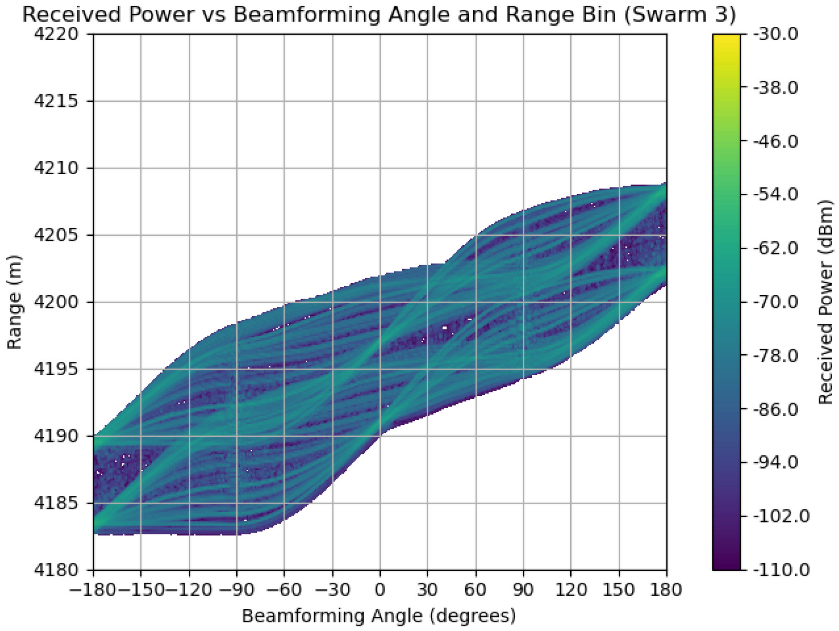

Figure 7: Range vs Azimuth angle for Swarm 3: Received Power.

The structure in each plot shows clearly the drawbacks of the choice of a 20ns linear frequency chirp for a target no more than 1m in any axis, as the illuminating waveform is 6 times longer than the target. The minimum bistatic range spread shown is 7m at -180 degrees beamforming angle. If a cross correlation function is used with the transmit chirp, this does produce a more defined range resolution response, as shown in Figure 8, Figure 9, & Figure 10, but due to the structure of the illumination function, this does not reduce the ranging error for each individual radar.

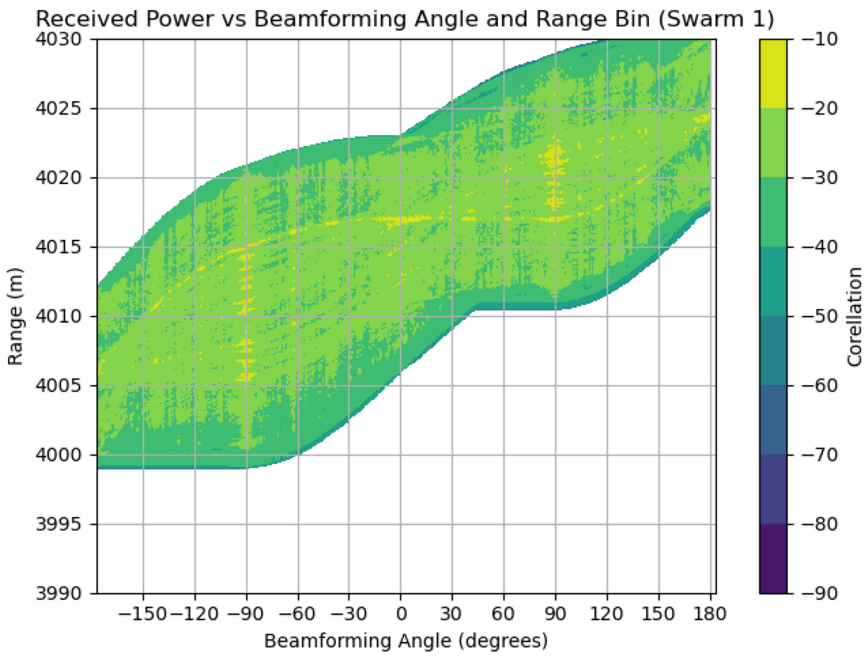

Figure 8: Range vs Azimuth angle for Swarm 1: Cross Correlation (dB).

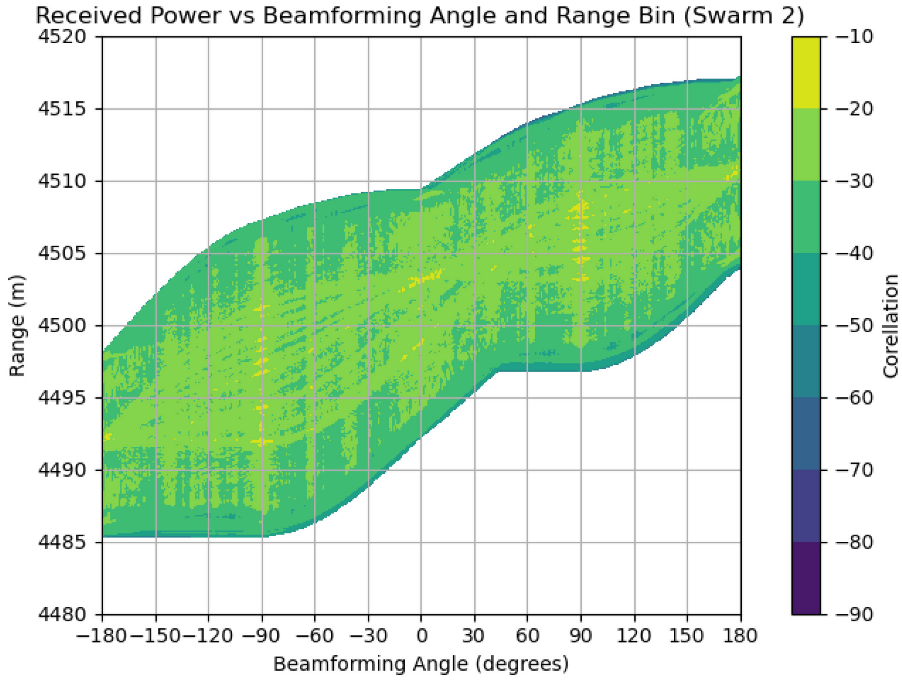

Figure 9: Range vs Azimuth angle for Swarm 2: Cross Correlation (dB).

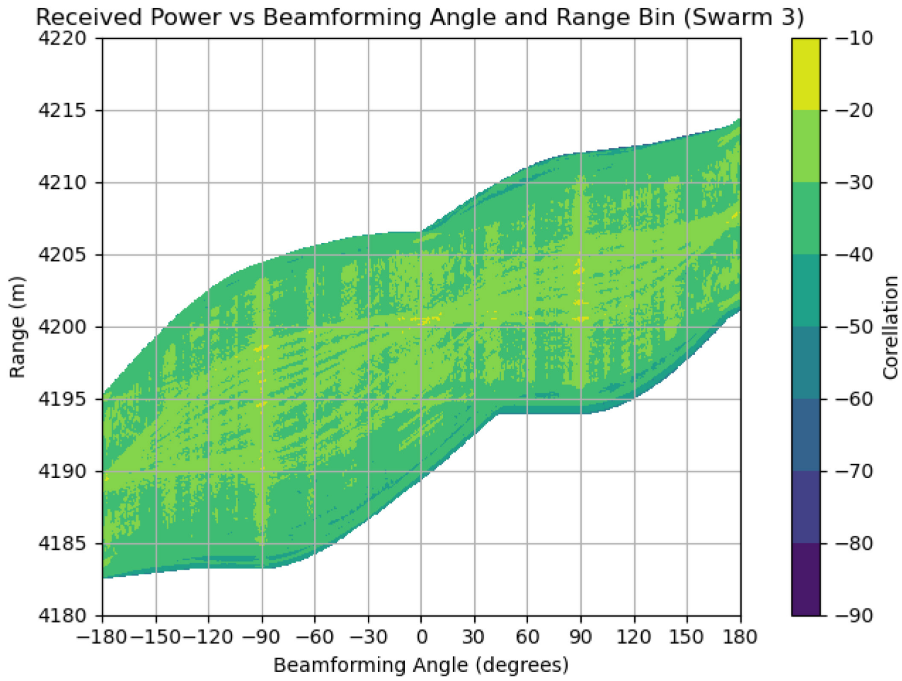

Figure 10: Range vs Azimuth angle for Swarm 3: Cross Correlation (dB).

The errors can be reduced using a multilateration approach, based upon the average range for the beamforming angle determined using angle of arrival analysis. This is shown in Figure 11, labelling each UAS in the swarm, and displaying their bistatic constant range isocontour in the same colour as their position indicator (Red-Swarm 1, Green-Swarm 2, Blue-Swarm 3). The true position of the target is shown using an aqua circle, and using mean square error cost function, minimized using Nelder-Mead optimization recovers predicts a final detected position 5.9m from the real target position, equivalent to the transmit pulse length.

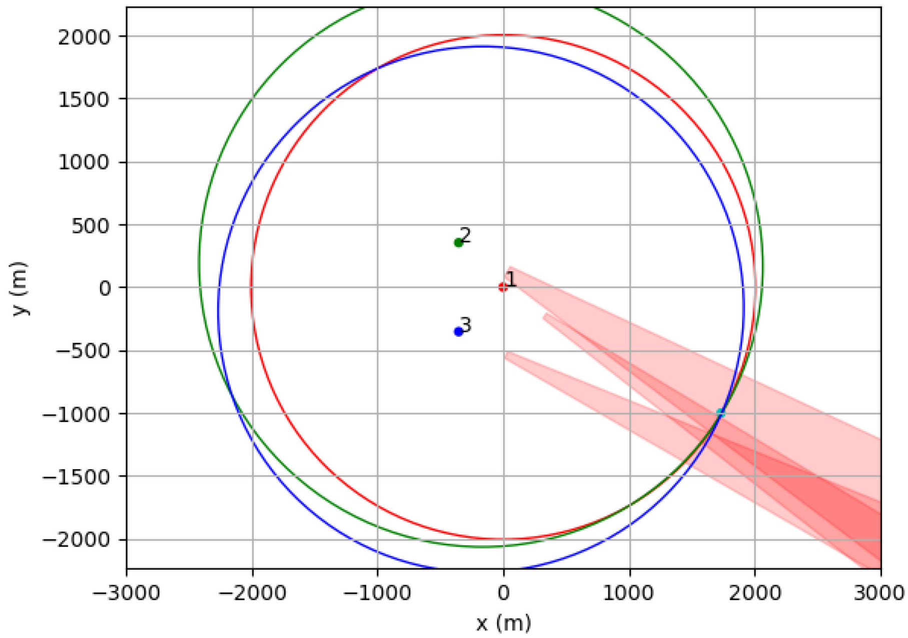

Figure 11: Multilateration Plot, showing 3dB power angle of arrival contours (red wedges), and bistatic equal range contours for each transmit-receiver pairing.

4.0 CONCLUSIONS

This work has proposed an opensource electromagnetics package supporting the modelling of multi-dimensional radar in both the frequency and time domain. This package includes support for the modelling of surveillance, tracking, and imaging radar. An example of swarm radar using three cooperative UAV with X band radar has been included, and the extent to which the output can be used to replicate realistic radar performance has been discussed. In the future, LyceanEM will continue to be developed in search of greater computational efficiency, support for velocity and doppler processing, and more complex propagation algorithms, supporting atmospheric losses, and imaging of lossy materials.

5.0 REFERENCES

[1] H. Griffiths and A. Farina, “Multistatic and {Networked} {Radar}: {Principles} and {Practice},” 2021 IEEE Radar Conf., pp. 1–5, 2021, doi: 10.1109/RadarConf2147009.2021.9455149.

[2] J. S. Herd and M. David Conway, “The Evolution to Modern Phased Array Architectures,” Proc. IEEE, vol. 104, no. 3, pp. 519–529, 2016, doi: 10.1109/JPROC.2015.2494879.

[3] A. Guerra, D. Dardari, and P. M. Djuric, "Dynamic Radar Network of UAVs: A Joint Navigation and Tracking Approach," IEEE Access, vol. 8, pp. 116454–116469, 2020, doi: 10.1109/ACCESS.2020.3001393.

[4] P. Hannan, "The Element-Gain Paradox for a Phased-Array," IEEE Trans. Antennas Propag., vol. 12, no. 4, pp. 423–433, 1964, doi: 10.1109/TAP.1964.1138237.

[5] M. Edrich and A. Schroeder, "Multiband multistatic Passive Radar system for airspace surveillance: A step towards mature PCL implementations," in 2013 International Conference on Radar, Sep. 2013, pp. 218–223, doi: 10.1109/RADAR.2013.6651988.

[6] M. Ben Kilani, G. Gagnon, and F. Gagnon, "Multistatic Radar Placement Optimization for Cooperative Radar-Communication Systems," IEEE Commun. Lett., vol. 22, no. 8, pp. 1576–1579, Aug. 2018, doi: 10.1109/LCOMM.2018.2837913.

[7] T. Counts, A. C. Gurbuz, W. R. Scott, J. H. McClellan, and K. Kim, "Multistatic Ground-Penetrating Radar Experiments," IEEE Trans. Geosci. Remote Sens., vol. 45, no. 8, pp. 2544–2553, Aug. 2007, doi: 10.1109/TGRS.2007.900677.

[8] P. Samczynski et al., "Air Target Imaging in Multichannel and Multistatic Passive Radars," in 2018 International Conference on Radar (RADAR), Aug. 2018, pp. 1–6, doi: 10.1109/RADAR.2018.8557309.

[9] H. Ren et al., "Swarm UAV SAR for 3-D Imaging: System Analysis and Sensing Matrix Design," IEEE Trans. Geosci. Remote Sens., vol. 60, pp. 1–16, 2022, doi: 10.1109/TGRS.2022.3221775.

[10] J. Li, P. Stoica, L. Xu, and W. Roberts, "On parameter identifiability of MIMO radar," IEEE Signal Process. Lett., vol. 14, no. 12, pp. 968–971, 2007, doi: 10.1109/LSP.2007.905051.

[11] E. Fishler, A. Haimovich, R. Blum, D. Chizhik, L. Cimini, and R. Valenzuela, "MIMO radar: An idea whose time has come," IEEE Natl. Radar Conf. - Proc., pp. 71–78, 2004, doi: 10.1109/nrc.2004.1316398.

[12] B. Yuan, Z. Jiang, J. Zhang, Y. Guo, and D. Wang, "A Self-Calibration Imaging Method for Microwave Staring Correlated Imaging Radar With Time Synchronization Errors," IEEE Sens. J., vol. 21, no. 3, pp. 3471–3485, Feb. 2021, doi: 10.1109/JSEN.2020.3025453.

[13] N. Ghazalli, A. Balleri, M. Jahangir, F. Colone, and C. J. Baker, "Passive Detection Using a Staring Radar Illuminator of Opportunity," 2019 Int. Radar Conf. RADAR 2019, Sep. 2019, doi: 10.1109/RADAR41533.2019.171344.

[14] C. S. Technologies, "Microwave Studio." Computer Simulation Technologies (CST), [Online]. Available: www.cst.com.

[15] Z. Cendes, "The development of HFSS," in 2016 USNC-URSI Radio Science Meeting (Joint with AP-S Symposium), USNC-URSI 2016 - Proceedings, Jun. 2016, pp. 39–40, doi: 10.1109/USNC-URSI.2016.7588501.

[16] D. C. Last et al., "Stone Soup: announcement of beta release of an open-source framework for tracking and state estimation," in Signal Processing, Sensor/Information Fusion, and Target Recognition XXVIII, 2019, vol. 11018, p. 6, doi: 10.1117/12.2518514.

[17] P. A. Thomas, J. Barr, B. Balaji, and K. White, “An open source framework for tracking and state estimation (‘Stone Soup’),” Signal Process. Sensor/Information Fusion, Target Recognit. XXVI, vol. 10200, p. 1020008, 2017, doi: 10.1117/12.2266249.

[18] T. Pelham, “Rapid {Antenna} and {Array} {Analysis} for {Virtual} {Prototyping},” Oct. 2022, [Online]. Available: https://radar2022.theiet.org/.

[19] T. Pelham, G. Hilton, E. Mellios, and R. Lewis, “Predicting Conformal Aperture Gain from 3D Aperture and Platform Models,” IEEE Antennas Wirel. Propag. Lett., vol. 1, no. 2, p. 1, 2016, doi: 10.1109/LAWP.2016.2600403.

[20] T. G. Pelham, “LyceanEM Examples: UAV and Antenna Array Beamforming Example.” https://lyceanem-python.readthedocs.io/en/latest/auto_examples/08_beamforming_architecture.html#sphx-glr-auto-examples-08-beamforming-architecture-py.

[21] W.-Q. Wang, C. Ding, and X. Liang, “Time and phase synchronisation via direct-path signal for bistatic synthetic aperture radar systems,” Iet Radar Sonar Navig., vol. 2, pp. 1–11, 2008, doi: 10.1049/IET-RSN:20060097.